Orbital: The Electronic Journal of Chemistry
journal homepage: www.orbital.ufms.br
ISSN 1984-6428

| Vol 9 | | No. 5 | | October-December 2017 |

Full Paper

Solvent Effect, Photochemical and Photophysical Properties of Phthalocyanines with Different Metallic Nuclei

Charles Biral Silva, Anderson Orzari Ribeiro, Hueder Paulo Moisés de Oliveira*

Federal University of ABC / Centro de Ciências Naturais e Humanas, Avenida dos Estados, 5001 – Santo André, São Paulo CEP 09210-580, Brazil

Article history: Received: 10 July 2017; revised: 10 November 2017; accepted: 13 November 2017. Available online: 24 December 2017. DOI: http://dx.doi.org/10.17807/orbital.v9i5.1047

Abstract: Photophysical and photochemical properties of lithium phthalocyanine (**1**), gallium(III) phthalocyanine chloride (**2**), titanium(IV) phthalocyanine dichloride (**3**) and iron(II) phthalocyanine (**4**) were investigated in dimethyl sulfoxide (DMSO), tetrahydrofuran (THF) and DMSO-THF mixtures. The influence of the central metal on these properties was analyzed according to solvent type, axial ligands and their paramagnetic and diamagnetic effect. Fluorescence lifetimes were recorded using a time correlated single photon counting setup (TCSPC) technique. In order to demonstrate the generation of reactive oxygen species under light irradiation, the indirect method (applying 1,3-diphenylisobenzofuran (DPBF) as chemical suppressor) and the direct method (analyzing the phosphorescence decay curves of singlete oxygen at 1270 nm) were employed. Compounds **1**, **2** and **3** showed a monomeric behavior in all media while compound **4** presented low aggregation in DMSO, but a very pronounced aggregation behavior in THF. Steady-state fluorescence anisotropy was compared with emission spectra and complex **4** presented values beyond the expected limits.

Keywords: metallic nuclei; phthalocyanines; single photon counting; singlet oxygen phosphorescence; solvent effect

1. INTRODUCTION

Phthalocyanines (Pcs) are aromatic macromolecules applied in numerous areas such as electrochromic displaying systems [1, 2], solar cells [3-5], optical storage devices [6] and photodynamic therapy (PDT) [7-9]. Chemical and physical properties of phthalocyanines may be modified by the nature of the substituents on the benzene rings or the nature of the axial ligand in the central metal [10]. As it is known, phthalocyanine compounds have high aggregation tendency due to their high π-π stacking interactions [11]. This feature hinders not only the solubility of compounds but also their photophysical, photochemical and spectroscopic properties in solution. Generally, aggregation depends on some factors, such as concentration, temperature, nature of the substituents, nature of the solvents and complexed metal ions [12, 13]. For example, large metals such as Aluminum (Al) and Indium (In) are able to hold axial ligands and diminish intermolecular interactions between macrocycles, therefore decreasing aggregation in solution.

The influence of central metal ions on the photophysical and photochemical parameters of benzothiazole-substituted phthalocyanines was investigated in tetrahydrofuran (THF) solution by Nas and co-workers [14]. The authors described a large red shift in the Q absorbance band attributed to highly deformed phthalocyanine skeleton by the large size of central lead ion, which did not fit into the cavity of phthalocyanine molecule. Additionally, the variety of metal ions in the framework of the Pc ring affects the fluorescence quantum yields and lifetime values of compounds.

Nas and co-workers [15] published a study on the photophysical and photochemical properties of oxadiazol tetra-substituted phthalocyanine with different metals. The aggregation behavior and electronic absorption spectra of the compounds were studied in different solvents (DMF, DMSO, chloroform, dichloromethane, THF and toluene). The unmetallated phthalocyanine compound showed no aggregation in chloroform, dichloromethane and THF. However, this compound formed aggregates in other used solvents, especially in DMSO, indicating the

*Corresponding author. E-mail: hueder.paulo@ufabc.edu.br

influence of the solvent effect. The ϕ_F values for unmetallated and zinc(II) oxadiazole substituted phthalocyanine were lower than those of unsubstituted zinc(II) phthalocyanine, suggesting more quenching due to the substitution and the interaction with the solvent.

The solubility and aggregation processes of peripherally/non-peripherally zinc and indium phenylphenoxy substitued phthalocyanines were investigated by Ali and co-workers [16]. They reported that the indium phthalocyanine derivative presents a red shifted Q-band when compared to the corresponding zinc phthalocyanine, in DMSO, suggesting a non-planar effect of a larger central indium atom. In addition, the indium phthalocyanine presented no fluorescence emission spectra as a mirror image of the excitation spectra, which can be attributed to the large indium atom in the cavity phthalocyanine macrocycle. The zinc phthalocyanine derivative showed strong fluorescence, while the indium macrocycles showed very low fluorescence emission due to the heavy metal atom effect.

Göksel [17] described the study of a new phthalocyanine biotin derivative to understand the influence of the biomolecule and heavy central metal atoms on the photophysical and photochemical properties. The UV–vis spectra of the compounds were obtained in different solvents and the results demonstrated that the aggregation behavior of the macrocycles was dependent on the concentration, nature of solvent, nature of substituents, complexed metal ions, and temperature. The fluorescence lifetime values of the substituted phthalocyanines were lower than the unsubstituted phthalocyanines in DMSO, suggesting more quenching due to the presence of heavy central metal atom.

In the present study, the aggregation behavior as well as photophysical and photochemical properties of four commercial metal phthalocyanines were investigated. The studied compounds (Figure 1) were di-lithium phthalocyanine **(1)**, gallium(III) phthalocyanine chloride **(2)**, titanium(IV) phthalocyanine dichloride **(3)** and iron(II) phthalocyanine **(4)**. These metals were chosen because of their different features. Lithium does not show any axial ligands and presents two metal ions, because of by the fact of the Li^+ be an alkaline metal, it is monovalent, and each metal atom interact with one of the central nitrogen atoms of macrocycle. Gallium and titanium show one and two axial ligands, respectively. Iron is a unique metal that presents paramagnetic behavior.

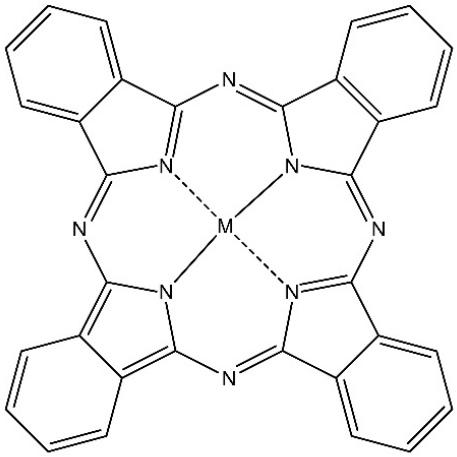

	1	2	3	4
M	Li	GaCl	$TiCl_2$	Fe

Figure 1. The chemical structure of the studied compounds **1-4.**

2. MATERIAL AND METHODS

2.1 Materials

The compound 1,3-diphenylisobenzofuran (DPBF) and the studied compounds di-lithium phthalocyanine **(1)**, gallium(III)-phthalocyanine chloride **(2)**, titanium(IV) phthalocyanine dichloride **(3)** and iron (II) phthalocyanine **(4)** as well as the standard zinc phthalocyanines (**ZnPc**) were purchased from Aldrich. Tetrahydrofuran (THF) and dimethyl sulfoxide (DMSO) were also purchased from Aldrich. Reagents were used as received without further purification and solvents were dried.

2.2 Equipment

UV-visible region absorption spectra were obtained with an Agilent Cary 60 UV-Vis Spectrophotometer. Fluorescence excitation and emission spectra were recorded on an Agilent Cary Eclipse Fluorescence Spectrophotometer using 1 cm path length quartz cuvette at room temperature. Fluorescence lifetimes (τ_F), Steady-State Fluorescence Anisotropy and Phosphorescence decay curves at 1270 nm were recorded on a PicoQuant FluoTime 300 Fluorescence Lifetime Spectrometer. Fluorescence lifetimes (τ_F) were recorded using a time correlated single photon counting setup (TCSPC). The decays

were analyzed by means of PicoQuant FluoFit Global Fluorescence Decay Analysis Software. Phosphorescence decay curves at 1270 nm were recorded in the equipment equipped with a near-infrared photomultiplier tube (NIR PMT) Hamamatsu, model H10330B. Photo-irradiations were done using a picosecond pulsed diode laser (LDH-P-635 driven by PDL 800-B, 635 nm, 80 MHz repetition rate, 72 ps pulse width, PicoQuant GmbH).

2.3 Sample preparation

All solutions were prepared by saturation and filtration. Compounds concentration were adjusted and all measurements were carried out at similar absorbance rate (~0.10-0.20). These conditions were chosen in order to avoid aggregated species. All study was carried out at room temperature.

2.4 Photophysical and photochemical parameters

2.4.1 Fluorescence lifetimes and steady-state fluorescence anisotropy

Fluorescence lifetimes (τ_F) were directly recorded using a time correlated single photon counting setup (TCSPC).

Steady-state fluorescence anisotropy spectra were obtained by changing the detection polarization on a fluorescence path parallel or perpendicular to the polarization of the excitation light (635 nm). Anisotropy [18] values were calculated according to the following Equation (1):

$$r = \frac{I_{\parallel} - G I_{\perp}}{I_{\parallel} + 2G I_{\perp}} \qquad (1)$$

where $I_{\parallel}$ and $I_{\perp}$ are the observed fluorescence intensities parallel (emission polarizer parallel to the polarized excitation) and perpendicular (emission polarizer perpendicular to the polarized excitation) to the electric vector of the excitation light, respectively. In the spectrometer, G is the G-factor.

2.4.2 Singlet oxygen quantum yields

Singlet oxygen quantum yield (ϕ_{Δ}) determinations were carried out using the direct method, and experiments were performed at room temperature in the same conditions. Sample absorbance was adjusted to 0.05 at 635 nm (the laser excitation wavelength used), and ϕ_{Δ} values were determined in the air in THF using Equation [19] (2),

$$\phi_{\Delta} = \frac{\phi_{\Delta}^{Std}}{A^{Std}} A \qquad (2)$$

where ϕ_{Δ}^{Std} is the singlet oxygen quantum yield for the standard unsubstituted ZnPc (ϕ_{Δ}^{Std} = 0.53 in THF) [20]; A and A^{Std} are the integral of phosphorescence emission curve of singlet oxygen in 1270 nm of the studied compounds (**1-4**) and standard compounds, respectively.

Furthermore, the chemical method using DPBF as a quencher was also employed. This method is largely used in the literature [13, 21-25]. However, the chemical method was only employed in order to demonstrate the generation of reactive oxygen species under light irradiation. Therefore, ϕ_{Δ} values were calculated solely for the direct method.

3. RESULTS AND DISCUSSION

3.1 UV-vis absorption spectra

The phthalocyanines studied have two typical and significant absorption bands in the UV-vis region. One of them is known as "B" or "Soret" band, at 275-389 nm, due to the transitions from the deeper π levels to the LUMO [26, 27]. The other characteristic band is known as "Q" band, at 600-720 nm, as a result of the transitions from the first excited state π-HOMO to π *-LUMO [28]. The electronic absorption spectrum of the studied compounds is shown in Figure 2. The narrow and sharp Q bands evidenced the monomeric behavior [29, 30] for compounds **1-3,** while FePc **(4)** presents an aggregation behavior.

The Q band of the lithium, gallium and titanium phthalocyanine complexes (**1-3**) presents a red-shifted in DMSO according to the central metal [25, 31]. This suggests the existence of non-planar effect with the size increment of the central atom, which was also observed in THF (Figure 3). Complex **1** revealed the presence of an extra band at 688 nm in THF. This band can be explained by the demetalation tendency of dilithium phthalocyanines [32].

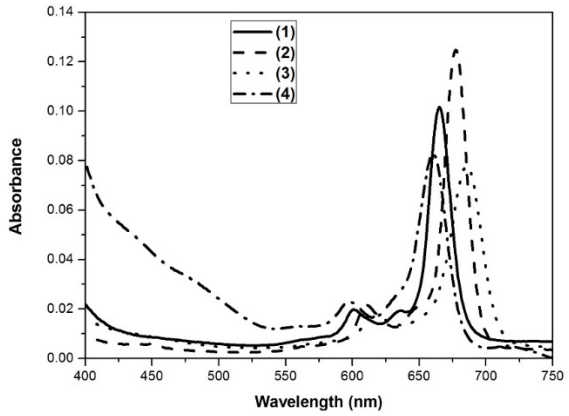

Figure 2. Absorption spectra of Li_2Pc (**1**), GaClPc (**2**), $TiCl_2Pc$ (**3**) and FePc (**4**) in DMSO.

The Q bands did not change extensively when the studied solvents were changed or proportionated, except for compound **3** (Figure 4 (A)). For this compound, the intensity in the B absorption band changes as the THF partition was increased, which may be because of the influence of the titanium metal, since the two axial ligands in the overlapping of the two sub bands (B1 and B2) [27]. This effect was not observed in the other compounds. Figure 4 (B) shows compound **2** as an example.

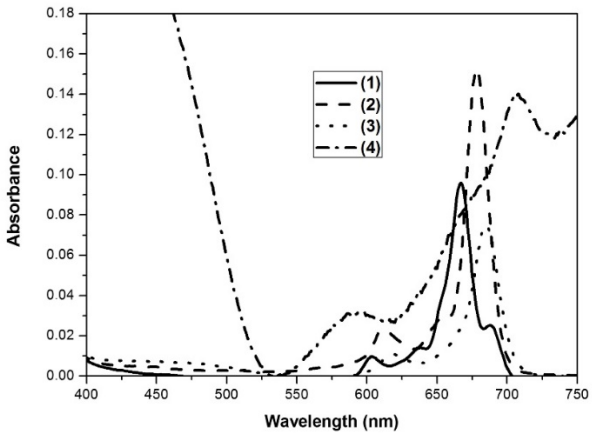

Figure 3. Absorption spectra of Li_2Pc (**1**), GaClPc (**2**), $TiCl_2Pc$ (**3**) and FePc (**4**) in THF.

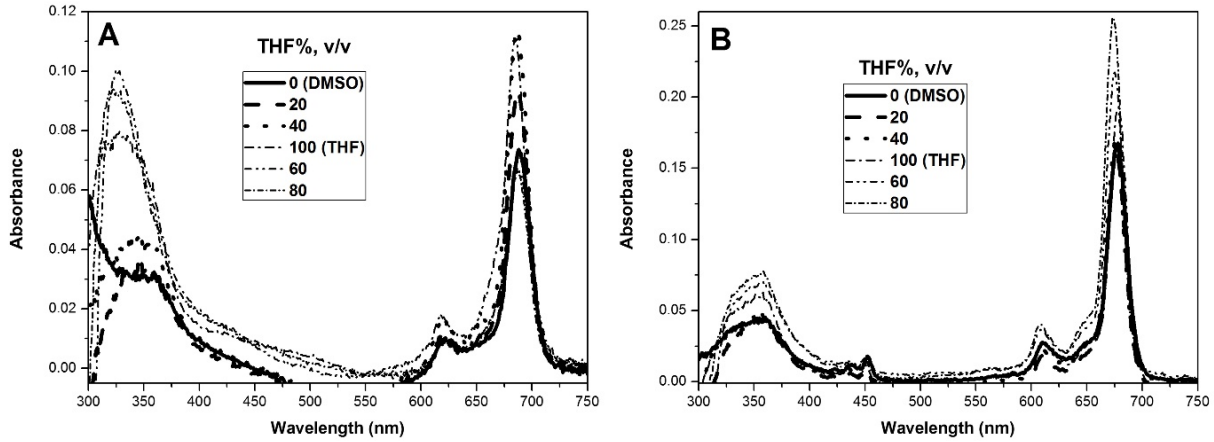

Figure 4. Absorption spectra of $TiCl_2Pc$ (**3**) (**A**) and GaClPc (**2**) (**B**) in the studied solvents and their mixtures.

3.2 Aggregation behavior

Aggregation behavior was explored in DMSO, $DMSO_{80\%}/THF_{20\%}$, $DMSO_{60\%}/THF_{40\%}$, $DMSO_{40\%}/THF_{60\%}$, $DMSO_{20\%}/THF_{80\%}$ and THF. All compounds were studied in similar intensity absorption at 670 nm. Figure 4 exhibits an example for complex **2** and **3**.

Compounds **1-3** presented no aggregation behavior in the studied solvents. Table 1 presents the maximum intensity wavelength in absorption and emission spectral, in all solvent conditions. On the other hand, compound **4** shows intense aggregation behavior when THF proportion was increased (Figure 5). This may be attributed to the lower coordinating ability of THF than DMSO with the central metal. The paramagnetic central ion also influences the absorption spectra and photophysical parameters [13, 25]. Similar intense single broaded Q bands of Iron (II) phthalocyanines are observed in other solvents as previously described [33, 34].

3.3 Fluorescence spectra

Fluorescence maximum wavelength, in all

solvent conditions studied, is listed in Table 1. The observed Stokes shifts were between 4-7 nm for complex **1**, 4-6 nm for complex **2** and 2-10 nm for complex **3**. Furthermore, the fluorescence spectra of the previously mentioned compounds were mirror images of their respective absorption spectra [35]. Absorption and emission spectra of the studied compounds are shown in Figure 6, in the same solvent conditions. Among compounds **1-3**, complex **3** presented the most significant Stokes shift. This may be due to the titanium metal ion and its two axial ligands out of the plane [33]. Complex **4** presented a different behavior compared to the other compounds, with larger Stokes shifts in DMSO, $DMSO_{80\%}/THF_{20\%}$ and $DMSO_{40\%}/THF_{60\%}$ (Figure 6).

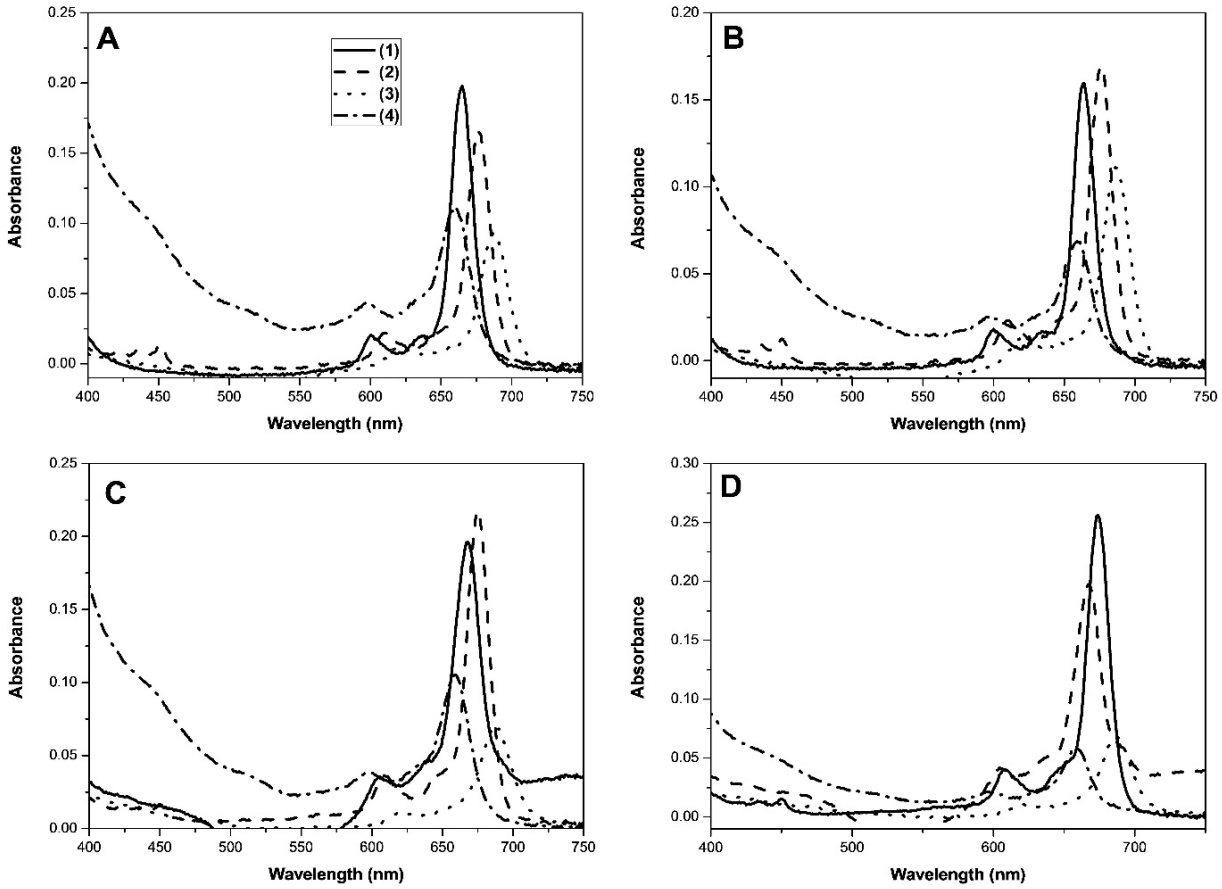

Figure 5. Absorption spectra of the studied compounds (**1-4**) in $DMSO_{80\%}/THF_{20\%}$ (**A**), $DMSO_{60\%}/THF_{40\%}$ (**B**), $DMSO_{40\%}/THF_{60\%}$ (**C**) and $DMSO_{20\%}/THF_{80\%}$ (**D**).

3.4 Lifetimes and anisotropy measurements

Fluorescence Lifetime determines the time available for the fluorophore to interact with its environment. The mean of lifetime is defined as the average time the molecule remains in the excited state until it returns to the ground state [36].

Values of τ_F are presented in Table 1. When comparing the studied compounds (**1-4**) in all solvent conditions, compound **1** has the largest τ_F value. In larger proportions of DMSO, the τ_F order is **1 > 2 > 3 > 4.** However, when THF proportion becomes higher, this order changes to **1 > 3 > 2 > 4**. These results show the influence of solvent on the metal phthalocyanines τ_F. Another solvent influence evidence is the change in lifetime values when the compounds were analyzed individually. The lifetime in compounds **1** and **3** increases when the THF amount increases. This fact suggests that the compounds are better solvated and stabilized in this media [37]. The opposite is observed for compound **2**. The decrease of τ_F in THF may be attributed to the small amounts of aggregates in the solution in addition to the solvent effect. The lifetime values for compound **4** are shorter than the other studied complexes. This behavior is already expected, once this complex showed aggregation behavior [13]

in studied conditions and has a paramagnetic metallic nucleus. However, complex **4** exhibited higher τ_F values in prevalence to THF media. When DMSO was absent, complex **4** presented higher τ_F values than complex **2**.

Table 1. Stokes shift, absorption and emission spectral data and fluorescence lifetime of studied compounds in DMSO, $DMSO_{80\%}/THF_{20\%}$, $DMSO_{60\%}/THF_{40\%}$, $DMSO_{40\%}/THF_{60\%}$, $DMSO_{20\%}/THF_{80\%}$ and THF.

Solvent	Compound	Q band λ_{max}, (nm)	Emission λ_{Em}, (nm)	Stokes Shift Δ_{Stokes}, (nm)	Stokes Shift Δ_{Stokes}, (cm^{-1})[a]	τ_F (ns)	χ^2
DMSO	**1**	666	673	7	156	4.69	0.994
	2	678	682	4	86	3.94	1.008
	3	688	698	10	208	3.57	1.085
	4	661	682[b]	21	465	2.28	1.248
$DMSO_{80\%}/THF_{20\%}$	**1**	665	670	5	112	4.83	1.089
	2	676	682	6	130	3.98	1.049
	3	687	696	9	188	3.68	0.995
	4	659	-	-	-	2.58	1.397
$DMSO_{60\%}/THF_{40\%}$	**1**	664	670	6	135	4.95	1.022
	2	676	682	6	130	3.94	1.023
	3	686	696	10	209	3.80	0.999
	4	659	676[b]	17	382	1.95	1.366
$DMSO_{40\%}/THF_{60\%}$	**1**	668	672	4	89	4.97	1.005
	2	675	679	4	87	3.66	0.988
	3	688	690	2	42	3.92	0.984
	4	659	678[b]	19	425	3.14	1.195
$DMSO_{20\%}/THF_{80\%}$	**1**	667	671	4	89	5.03	1.050
	2	674	678	4	87	3.35	1.015
	3	687	691	4	84	4.08	0.980
	4	659	-	-	-	2.96	1.088
THF	**1**	666	672	6	134	5.03	1.014
	2	679	684	5	108	2.40	1.015
	3	686	690	4	84	4.33	1.060
	4	708	-	-	-	2.90	1.089

[a] Values of Δ_{Stokes} calculated using wavenumber = $1 / \lambda \times 1x10^7$.
[b] Show no mirror images.

Steady-state fluorescence anisotropy was compared with emission spectra of the studied compounds (Figure 7). In complex **1,** positive regions appear interspersed with negative regions in almost all solvents, with the exception of $DMSO_{20\%}/THF_{80\%}$ and THF, which did not show anisotropy in emission region. For the media that presented anisotropy, *r* values ranged from -0.1 to 0.1. Complex **2** presented the same behavior, although just THF did not present anisotropy. Complex **3** showed anisotropy values in all studied media, but with *r* values ranging from -0.4 to 0.4, reaching the limiting anisotropy values [38]. Complex **4** was studied in DMSO, $DMSO_{60\%}/THF_{40\%}$ and $DMSO_{40\%}/THF_{60\%}$ because of the previously mentioned aggregation behavior. However, *r* values extrapolated the limits of the anisotropy value

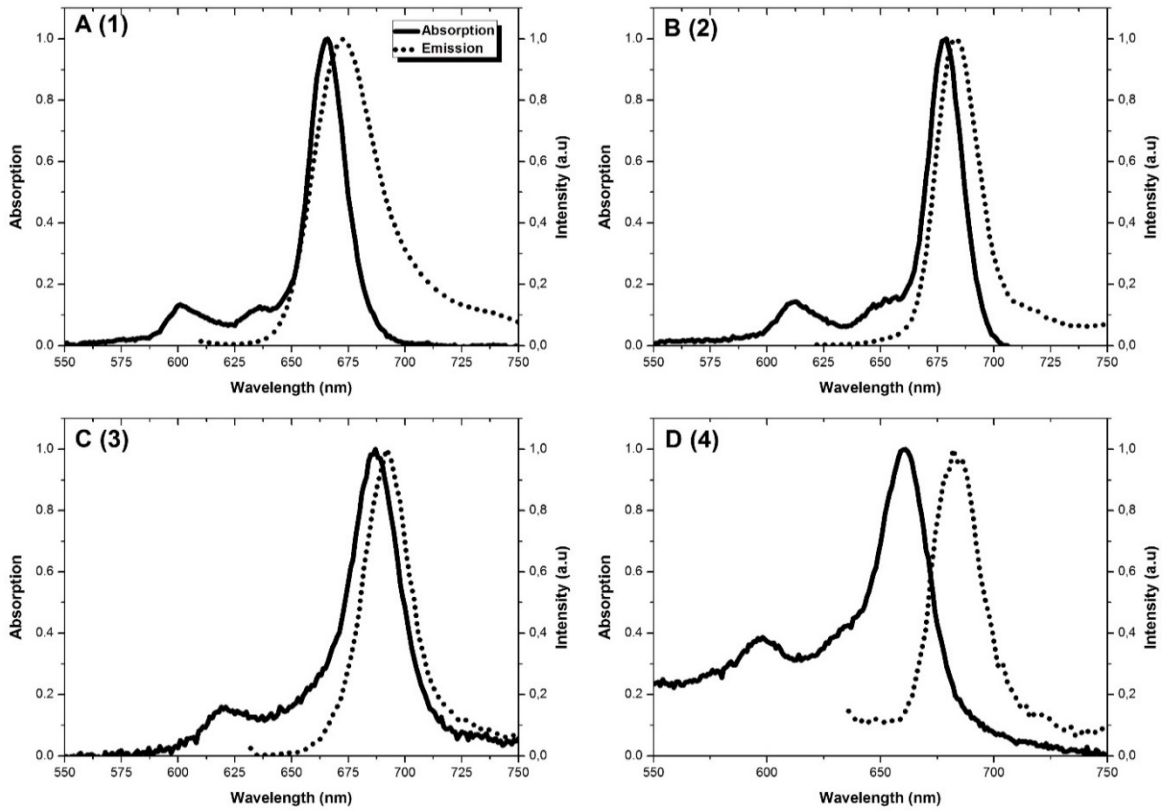

Figure 6. Absorption and emission spectra of Li_2 (**1**), Ga(III) (**2**), Ti(IV) (**3**) and Fe(II) (**4**) phthalocyanine compounds in DMSO (**A**), THF (**B**), $DMSO_{20\%}/THF_{80\%}$ (**C**) and DMSO (**D**).

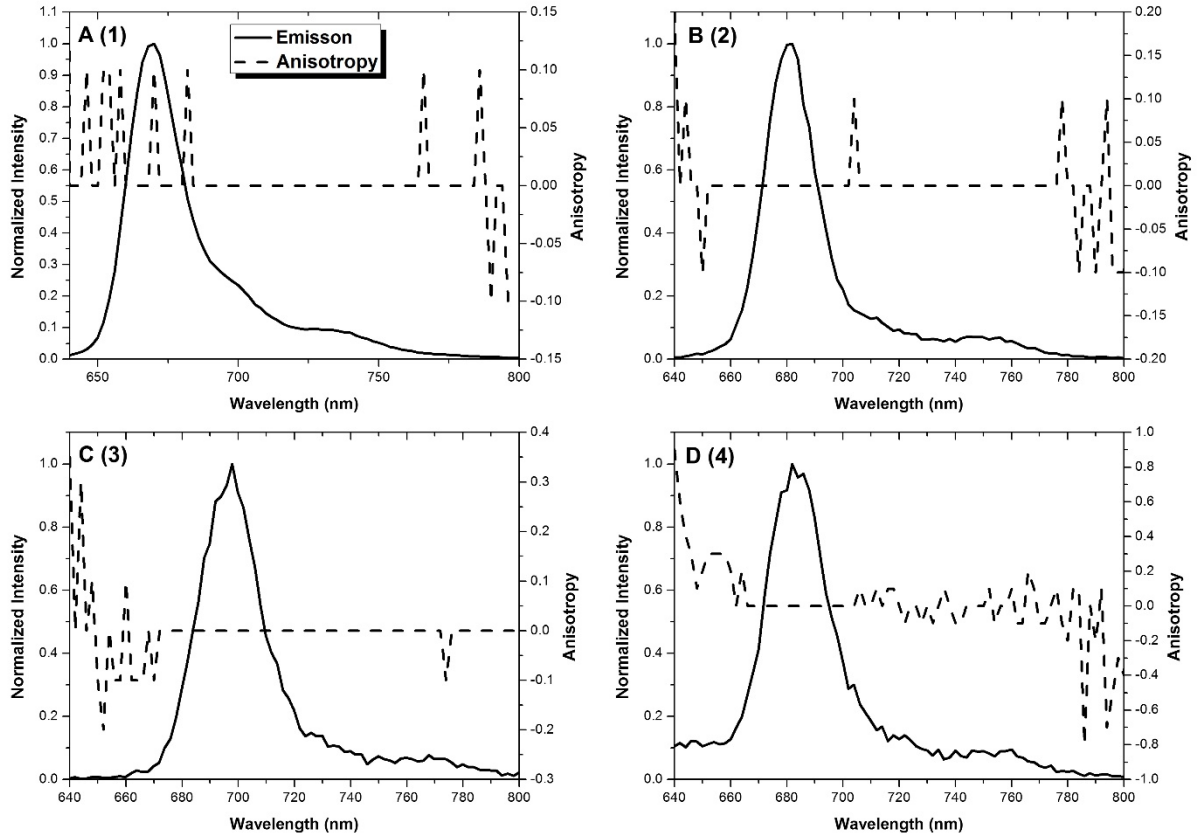

Figure 7. Emission spectra and steady-state fluorescence anisotropy of Li_2 (**1**), Ga(III) (**2**), Ti(IV) (**3**) and Fe(II) (**4**) phthalocyanine compounds in $DMSO_{60\%}/THF_{40\%}$ (**A and B**) and DMSO (**C and D**).

3.5 Singlet oxygen generation

Singlet oxygen (1O2) is the main species responsible for killing diseased cells in the treatment of tumor cancers by Photodynamic Therapy [39]. In the literature [23], it is reported that paramagnetic metals, such as copper and cobalt, have short-lived triplet states and consequently low singlet oxygen generation. However, phthalocyanines with diamagnetic metals, such as zinc (Zn^{2+}), aluminum (Al^{3+}), gallium (Ga^{3+}) and silicon (Si^{4+}) [9, 24] have long triplet lifetimes and consequently better singlet oxygen generation. The paramagnetic feature not only influences photochemical parameters, but also photophysical properties [25]. Studies of triplet lifetimes were not carried out, although it is known that lithium, gallium and titanium have generally good triplet lifetimes through previous studies [40-42].

In order to demonstrate the generation of reactive oxygen species under light irradiation [43-44], we employed the chemical method using DPBF as a quencher. In this method, UV-vis spectra were obtained to monitor the disappearance of DPBF absorbance at 417 nm. The results for complex **2** is shown in DMSO (A) and THF (B) in Figure 8.

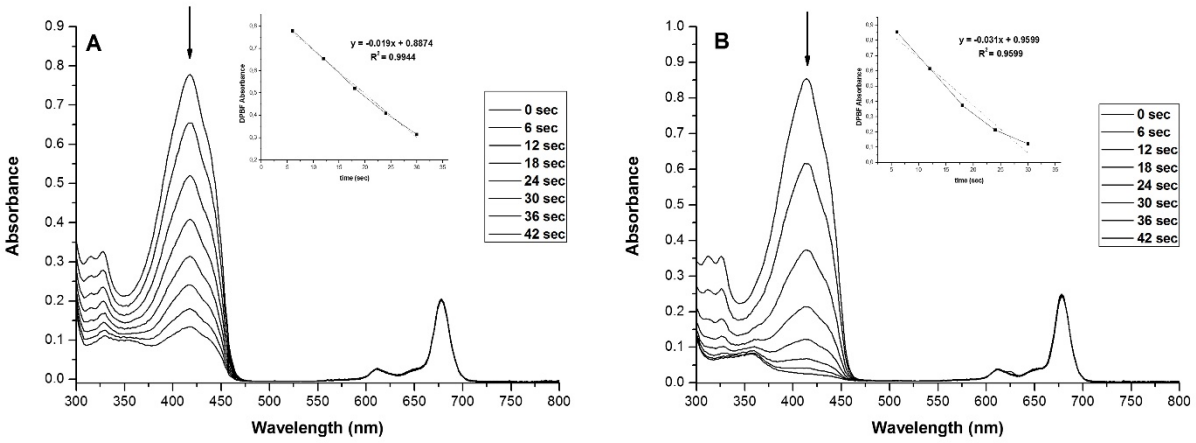

Figure 8. UV-vis spectra of solution containing complex **2** in DMSO (**A**) and THF (**B**) and the changes in DPBF, under constant irradiation by red LED light obtained after each six-second irradiation period. (Inset: Plot of DPBF absorbance versus time).

The consumption of DPBF is shown for all studied compounds in DMSO (A) and THF (B) as seen in Figure 9. Compound **4** does not generate singlet oxygen expressively in either solvent. Other compounds (**1-3**) are capable of generating considerable amounts of singlet oxygen.

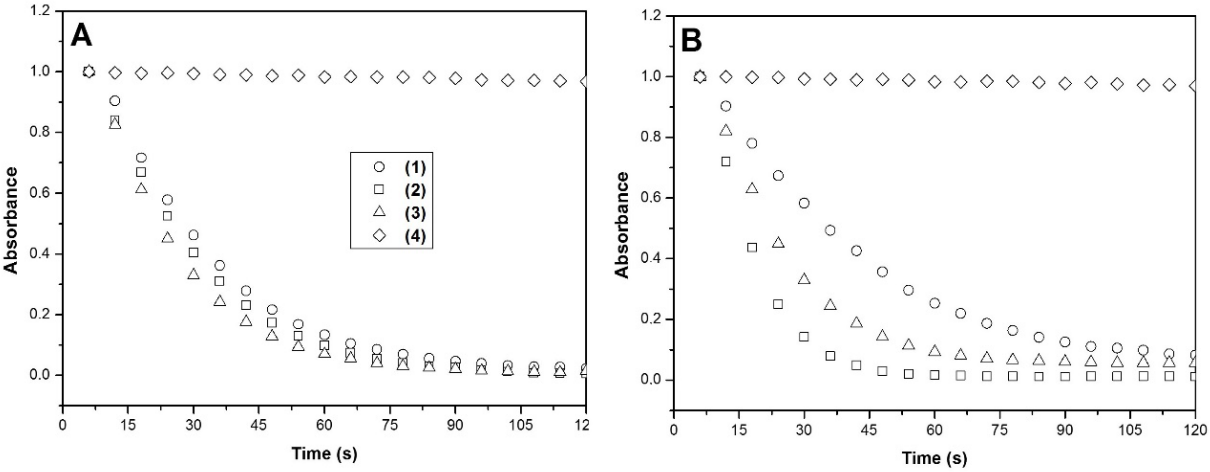

Figure 9. DPBF consumption of studied compounds in DMSO (**A**) and THF (**B**).

Rate constants were calculated in relation of DPBF consumption. The constants are in accordance with Figure 9, where k = 0.037 s^{-1} for compound **1**, k = 0.043 s^{-1} for **2**, k = 0.049 s^{-1} for **3** in DMSO and k = 0.025 s^{-1} for **1,** k = 0.076 s^{-1} for **2** and k = 0.044 s^{-1} for **3** in THF. As expected, the rate constant for compound **4** was almost null (approximately 2.0 x 10^{-4} s^{-1}).

Also, the singlet oxygen quantum yield (ϕ_Δ) was determined using the direct method, which analyzes phosphorescence decay curves at 1270 nm using NIR PMT accessory. The ϕ_Δ values cannot be obtained in DMSO [45] and the values were obtained only in pure THF. Decay curves are represented in Figure 10.

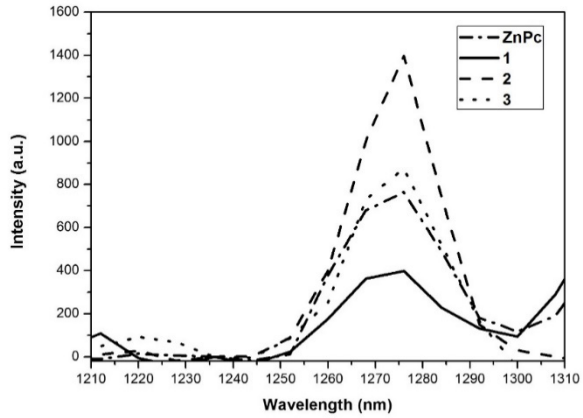

Figure 10. Phosphorescence decay curves at 1270 nm of singlet oxygen.

The ϕ_Δ value of compound **1** (LiPc) was determined as ϕ_Δ = 0.44, compound **2** (GaClPc) as ϕ_Δ = 0.63, and compound **3** ($TiCl_2Pc$) as ϕ_Δ = 0.57. These values correspond with phosphorescence decay curves. Compound **4** (FePc), as expected, was unable to generate singlet oxygen in quantitative amounts. These values are in agreement with DPBF consumption as observed in Figure 9 (B). Compounds **2** and **3** presented higher values of ϕ_Δ than the standard compound (ϕ_Δ = 0.53). All studied central metal ions are able to generate appreciable singlet oxygen amounts, with exception of compound **4,** due to the paramagnetic behavior.

4. CONCLUSION

The aggregation behavior of the studied compounds was investigated in DMSO, THF and DMSO-THF mixtures. Compounds **1**, **2** and **3** showed a monomeric behavior in all media. This evidence is supported by single and narrow Q band. Compound **4** presented low aggregation in DMSO, but a very pronounced change in this behavior was observed in THF. The photophysical results showed the influence of central metal ion on fluorescence lifetime values. Complex **4** presented the lowest values due to the presence of aggregate species in the studied solvents, besides the paramagnetic feature of complex metal ion. When DMSO was the main solvent, the τ_F order is **1 > 2 > 3 > 4.** However, when THF proportion becomes higher, this order changes to **1 > 3 > 2 > 4**. The influence of solvent in photophysical media was observed. The lifetime in compounds **1** and **3** increases significantly when the THF amount increases and this fact suggests better solvated and stabilized in this media of these compounds. Steady-state fluorescence anisotropy was compared with emission spectra and complex **4** presented values beyond the expected limits. Complex **1-3** presented high quantum generation yield of singlet oxygen, which demonstrated that these metals are recommended to photodynamic therapy.

5. ACKNOWLEDGMENTS

The authors would like to thank FAPESP (2014/18527-8), CNPq (474019/2012-8 and 402289/2013-7) for their financial support, Complexo Laboratorial Nanotecnológico da UFABC and PicoQuant GmbH.

6. REFERENCES AND NOTES

[1] Mckeown, N. B. Phthalocyanine Materials: Synthesis, Structure and Function. Cambridge University Press, Cambridge, 1998.

[2] Leznoff, C.C., Lever, A. B. P. Phthalocyanines Properties and Applications, vol. 3, VCH Publisher, New York, 1993.

[3] Taffa, D. H.; Kathiresan, M.; Arnold, T.; Walder, L.; Erbacher, M. Bauer, D. *J. Photochem. Photobiol. A.* **2010**, *216,* 35. [CrossRef]

[4] Kushto, G. P.; Mäkinen, A. J.; Lane, P.A. *IEEE J. Sel. Top. Quantum Electron,* **2010**, *16*, 1552. [CrossRef]

[5] Yang, F.; Forrest, S. R. *ACS Nano,* **2008**, *2,* 1022. [CrossRef]

[6] Emmelius, M.; Pawlowski, G.; Vollmann, H. W. *Angew. Chem. Int.* **1989**, *28*, 1445. [CrossRef]

[7] Rosenthal, I. *Photochem. Photobiol.,* **1991**, *53,* 859. [CrossRef]

[8] Leznoff, C. C.; Lever, A. B. P. Phthalocyanines, Properties and Applications, vol. 4, VCH Publisher, New York, 1996.

[9] Maduray, K.; Odhav, B. *J. Photochem. Photobiol. B.* **2013**, *128,* 58. [CrossRef].

[10] Saka, E. T.; Göl, C.; Durmus, M.; Kantekin, H.; Biyiklioglu, Z. *J. Photochem. Photobiol. A.,* **2012**, *241,* 67. [CrossRef]

[11] Martínez-Díaz, M. V.; Rodríguez-Morgade, M. S.; Feiters, M. C.; van Kan, P. J. M.; Nolte, R. J. M.; Stoddart, J. F.; Torres, T. *Org. Letters,* **2000**, *2*, 1057. [CrossRef]

[12] Dominguez, D. D.; Snow, A. W.; Shirk, J. S.; Pong, R. G. S. *J. Porphy. Phthalocyan.* **2001**, *5*, 582. [CrossRef]

[13] Çakır, D.; Çakır, V.; Biyiklioglu, Z.; Durmus, M.; Kantekin, H. *J. Organ. Chem.* **2013**, *745-746,* 423. [CrossRef]

[14] Nas, A.; Dilber, G.; Durmus, M.; Kantekin, H. *Spectrochim. Acta, Part A.* **2015**, *135*, 55. [CrossRef]

[15] Nas, A.; Kantekin, H.; Durmus, M.; Gumrukçuoglu, N. *J. Lumin.* **2014**, *154*, 15. [CrossRef]

[16] Ali, H. E. A.; Piskin, M.; Altun, S.; Durmus, M.; Odabas Z. *J. Lumin.* **2016**, *173,* 113. [CrossRef]

[17] Göksel M. *Bioorg. Med. Chem.* **2016**, *24,* 4152. [CrossRef]

[18] Jia, M.; Ma, X.; Yan, L.; Wang, H.; Guo, Q.; Wang, X. *J. Phys. Chem. A.* **2010**, *114*, 7345. [CrossRef]

[19] Bonacin, J. A.; Engelmann, F. M.; Severino, D.; Toma, H. E.; Baptista, M. S. *J. Braz. Chem. Soc.* **2009**, *20,* 31. [CrossRef]

[20] Gümrükçü, G.; Karaoglan, G. K.; Erdogmus, A.; Gül, A.; Avciata, U. *J. Chem.* **2014**, *2014,* 1. [CrossRef]

[21] Seotsanyana-Mokhosi, I.; Kuznetsova, N.; Nyokong, T. *J. Photochem. Photobiol. A*. **2001**, *140,* 215. [CrossRef]

[22] Ramos, A. A.; Nascimento, F. B.; de Souza, T. F. Omori, A. T.; Manieri, T. M.; Cerchiaro, G.; Ribeiro, A. O. *Molecules* **2015**, *20,* 13575. [CrossRef]

[23] Chauke, V.; Ogunsipe, A.; Durmus, M.; Nyokong, T. *Polyhedron* **2007**, *26*, 2663. [CrossRef]

[24] Durmus, M.; Nyokong, T. *Inorg. Chem. Comm.* **2007**, *20*, 332. [CrossRef]

[25] Bayrak, R.; Akçay, H. T.; Piskin, M.; Durmus, M. Degirmencioglu, I. *Dyes Pigments* **2012**, *95*, 330. [CrossRef]

[26] Stillman, M. J.; Nyokong T. in: C. C. Leznoff, A. B. P. Lever (Eds.). Phthalocyanines: Properties and Applications, vol. 1, VCH Publisher, New York, 1989 (Chapter 3).

[27] Değirmencioğlu, İ.; Bayrak, R.; Er, M.; Serbest, K. *Dyes Pigments* **2009,** *83*, 51. [CrossRef]

[28] Ueno, L. T.; Jayme, C. C.; Silva, L. R.; Pereira, E. B.; de Oliveira, S. M.; Machado, A. E. H. *J. Braz. Chem. Soc.* **2012**, *23,* 2237. [CrossRef]

[29] Sessler, J. L.; Jayawickramarajah, J.; Gouloumis, A.; Pantos, G. D.; Torres, T. *Tetrahedron* **2006**, *62*, 2123. [CrossRef]

[30] Biyiklioglu, Z.; Çakir, D. *Spectrochim. Acta Part A: Molec. Biomolec. Spectrosc.* **2012**, *98*, 178. [CrossRef]

[31] Demirbaş, Ü.; Bayrak, R.; Pişkin, M.; Akçay, H. T.; Durmuş, M.; Kantekin, H. *J. Org. Chem*. **2013,** *724*, 225. [CrossRef]

[32] Martin, K. A.; Stillman, M. J. *Inorg. Chem.* **1980**, *19*, 2473. [CrossRef]

[33] Saka, E. T.; Biyiklioglu, Z. *J. Organ. Chem.* **2013**, *745-746*, 50. [CrossRef]

[34] Zanguina, A.; Bayo-Bangoura, M.; Bayo, K.; Ouedraogo, G. V. *Bull. Chem Soc. Ethiop.* **2002**, *16*, 73. [CrossRef]

[35] Anslyn, E. V.; Dougherty, D. A. Modern Physical Organic Chemistry, vol. 1, University Science Books, California, 2005 (Chapter 16).

[36] Lakowicz, J. R. Principles of Fluorescence Spectroscopy. Ed. 3, Baltimore, Springer, 2006.

[37] Wang, T.; Zhang, X.-F.; Lu, X. *J. Mol. Struct.* **2015**, *1084*, 319. [CrossRef]

[38] Stanley, C.F. Photophysical evaluation of substituted zinc phthalocyanines as sensitisers for photodynamic therapy. *Durham theses,* Durham University, 1997. Available at Durham E-Theses Online: http://etheses.dur.ac.uk/4681/

[39] Niedre, M.; Patterson, M. S.; Wilson, B. C. *Photochem. Photobiol.* **2002**, *75,* 382. [CrossRef]

[40] Chen Y. *J. Mater. Sci.* **2006**, *41*, 2169. [CrossRef]

[41] Canlica, M.; Nyokong, T. *Polyhedron* **2011**, *30,* 1975. [CrossRef]

[42] Gilat, S. L.; Ebbesen, T. W. *J. Phys. Chem.* **1993**, *97,* 3551. [CrossRef]

[43] Castano, A. P.; Demidova, T. N.; Hamblin, M. R. *Photodiag. Photodyn. Ther.* **2005**, *1*, 279. [CrossRef]

[44] Durmus, M.; Nyokong, T. *Photochem. Photobiol. Sci.* **2007**, *6*, 659. [CrossRef]

[45] Gürel, E.; Peskin, M.; Altun, S.; Odabas, Z.; Durmus, M. *J. Photochem. Photobiol. A.* **2016**, *315*, 42. [CrossRef]